Nigerian Journal of Theoretical and Environmental Physics (NJTEP)
ISSN Print: 3026-9601
DOI: https://doi.org/10.62292/njtep.v1i1.2023.15
Volume 1(1), December 2023

Determination of Onset and End of Growing Season in Nigeria using the Modified Dynamic (Optimal) Threshold Method and Satellite data

***[1]Tertsea Igbawua, [2]Fanan Ujoh, [3]Grace Adagba, [1]Sylvester Gaando, [3]James Orduen Tsor**

[1]Department of Physics, Joseph Sarwua Tarka University, Makurdi, Benue State
[2]Centre for the Integrated Delivery of the Built Environment (IDoBE), School of the Built Environment and Architecture, London South Bank University, UK.
[3]Department of Physics, Benue State University, Makurdi, Benue State.

[*]Corresponding author's email: tertsea.igbawua@uam.edu.ng

ABSTRACT
Understanding and accurately determining the onset and end of the growing season is essential for crop management, forecasting yields, and assessing the impacts of climate change, which are crucial for various sectors such as agriculture, ecology, and climate science. The study investigates the start and end of seasons using the optimal threshold method in different climate zones from 2001 to 2022. The climate zones include Tropical Rainforest (Af), Tropical Monsoon (Am), Tropical Wet (Aw), Hot Semi-Arid (BSh), Hot Arid (BWh), and Hot Summer Mediterranean climates. The relationship between climate parameters (temperature and precipitation) and phenology was examined using cross-correlation analysis. Furthermore, the research explores the annual distribution of precipitation and temperature, highlighting the variable nature of precipitation compared to temperature. Climate zone-specific analyses reveal trends in precipitation and temperature changes, indicating potential impacts on vegetation growth. The results show that the Af (BWh) climate zone indicated the longest (shortest) season length, and longer zones with a larger Length of Season (LOS) experienced delayed End of Season (EOS) and/or an early onset of the season. Moreover, Af climate seasons start earlier and finish later than those in the other climate zones. The findings have shown that season length (LOS) in Af, Aw, BSh, BWh, and Csb increased at 1.2, 0.4, 0.2, 0.9, and 0.5 days/yr, respectively. However, it is noteworthy that Am experiences a contraction at -0.6 days/yr. The study found that climatic fluctuation has an impact on vegetation phenology throughout all climate zones of Nigeria. Changes in agricultural growing seasons should be studied to maximize agricultural output.

Keywords:
Vegetation phenology,
SOS & EOS,
Climate change,
Modified dynamic (optimal) threshold method,
Koppen climate zones.

INTRODUCTION

Vegetation phenology refers to the recurring timing of key plant life cycle events such as germination, defoliation, flowering, and senescence, which reflect small shifts that are important for plant function, ecosystem services, and their subsequent biophysical and biogeochemical interactions with the climate system (Chen *et al*. 2023). Temperature, rainfall, and human activities all influence phenological events, which affect plant growth and canopy functions, with temperature and rainfall sensitivity varying across different locations (Workie and Debella, 2018).

The growing season marks the period when environmental conditions are conducive to plant growth, influencing agricultural productivity, ecosystem dynamics, and carbon cycling. Understanding and accurately determining the onset and end of the growing season is essential for crop management, forecasting yields, and assessing the impacts of climate change, crucial for various sectors such as agriculture, ecology, and climate science. Generally, crop phenological information is mainly derived through three methods: Ground observation; Retrieval from web camera networks; and Retrieval from satellite times-series data (Huang *et al*., 2019; Li *et al*., 2023). Additionally, the start of season (SOS) and the end of season (EOS) are the most important among all vegetation phenological parameters given that all other parameters (e.g. length of season, etc.) are derived from SOS and EOS (Curnel & Oger, 2006).

Several studies have examined the dynamic link between vegetation phenology and climate change in a number of studies conducted in different locations. Wang *et al*. (2016) examined satellite-derived Normalized Difference Vegetation Index (NDVI) data for the Northern Hemisphere from 1982 to 2012. Their research showed that high latitude regions have longer growing seasons, mostly as a result of early plant development. Notably, during the course of the three decades, there was no discernible pattern in the heights of the vegetative growth seasons. A similar investigation by Jeong *et al*. (2011) looked at temperate vegetation in the Northern Hemisphere between 1982 and 2008. Their examination of temperature and NDVI data revealed an overall rise in growing season length. But there were subtle differences in the patterns of the SOS and the EOS of these seasons; SOS advanced more in the early era (1982-1999) than in the later period (2000-2008). Huang *et al*., (2019) investigate the optimal thresholds for retrieving the start of the season (SOS) and the end of the season (EOS) of different crops, and (2) compare the performances of the NDVI and Enhanced Vegetation Index (EVI) in retrieving crop phenology with a modified version of the dynamic threshold method. The outcome revealed that: first, the modification adopted ensured a 100% retrieval rate; second, it was inappropriate to retrieve SOS and EOS with the same threshold for all crops; and, third, for some crops, the accuracies of the SOS estimations based on EVI were generally higher compared to those based on NDVI.

Studies show that a variety of methods have been developed to extract vegetation phenological parameters from vegetation index time series. These include the fixed threshold method (Fisher, 1994; Lloyd, 1990), the dynamic threshold method (Jonsson & Eklundh, 2002; White *et al*., 1997), the moving average method (Duchemin *et al*., 1999; Reed *et al*., 1994), the function fitting method (Beck *et al*., 2006; Zhang *et al*., 2003), the maximum-slope method (Sakamoto *et al*., 2005), the valley detection method (Atkinson *et al*., 2012; Atzberger & Eilers, 2011), and the double logistic method (Fisher *et al*., 2006; Beck *et al*., 2006). The dynamic threshold method has been found advantageous among these methods because it requires less parameters, it has ease of application and guarantees high accuracy (Huang *et al*., 2019). It is for these reasons that contemporary studies adopt the dynamic threshold method for retrieving vegetation SOS and EOS. In Nigeria, Igbawua *et al*. (2023) assessed phenology metrics in different ecological zones using inflexion point method and results indicated variation in start, end, length and peak of seasons in the zones.

Traditionally, the onset and end of the growing season have been determined using fixed thresholds based on temperature or vegetation indices. However, these fixed thresholds may not adequately capture the variability in climate and vegetation dynamics, leading to inaccuracies in the estimation of growing season timings. To address this issue, the modified dynamic threshold method, also known as the optimal threshold method, has emerged as a promising approach for accurately identifying the onset and end of the growing season. This method accounts for the temporal variability in climate and vegetation conditions by dynamically adjusting the threshold based on historical data.

In this paper, we introduce the modified dynamic threshold method for determining the onset and end of the growing season in Nigeria. The choice of this method is based on its underlying principles, its advantages over traditional fixed threshold and other approaches, and its applications in various fields. Additionally, we assess the relationship between climate and phenology (onset, peak, length, and end of season) and also provide an overview of the computational techniques and data sources commonly used in implementing this method. By adopting the modified dynamic threshold method, researchers and practitioners can improve the accuracy of growing season timing estimates, leading to better-informed decision-making in agriculture, ecology, and climate science. This paper aims to contribute to the understanding and adoption of this innovative approach in the study of growing season dynamics specifically in Nigeria where conflicts between farming and grazing populations are beginning to continually escalating due to climate-induced pressures on availability of vegetation and land resources.

MATERIALS AND METHODS

Study Area

Nigeria is an African country comprised of 36 states and the Federal Capital Territory (Abuja). Situated between the dry Sahel and the desert to the north and the Atlantic Ocean to the south, the nation boasts an estimated land size of 923,769 km², positioned between latitudes 4°–14°N and longitudes 2°W–14°E. Nigeria encompasses diverse landscapes and undergoes varying climatic conditions across its regions. The country exhibits a range of Köppen climate zones, including Tropical Rainforest (Af), Tropical Monsoon (Am), Tropical Wet (Aw), Hot Semi-Arid (BSh), Hot Arid (BWh), and Hot Summer Mediterranean climates. In the southern regions, such as the Niger Delta, the climate falls within the Af, Aw, and part of Am zones, characterized by distinct wet and dry seasons. Generally, there is variation in the duration of the dry and wet seasons across the country, with the northern parts experiencing longer dry months and the southern parts having longer wet months. Figure 1 depicts the study area with

Köppen climate classifications (Chen and Chen, 2013) and Nigerian (NGA) states.

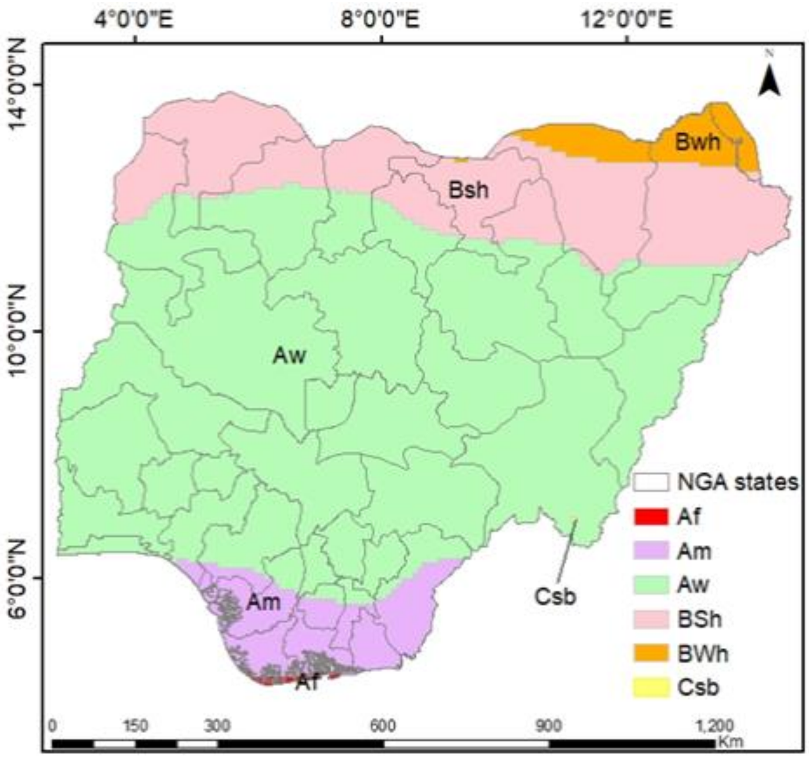

Figure 1: Map of Nigeria showing different climate zones

Data

The data used in this work include (1) Moderate Resolution Imaging Spectroradiometer (MODIS) Normalized Difference Vegetation Index (NDVI) satellite data. The MODIS Terra daily NDVI is derived from the MODIS/006/MOD09GA surface reflectance composites, available at https://lpdaac.usgs.gov/products/mod09gav006/. The Maximum Value Composite (MVC) method was used to aggregate the daily grid values into monthly values. The temporal range considered was from 2001 to 2022. Additionally, (2) Climate Research Unit (CRU) precipitation and temperature records from 2001 to 2022 were assessed at https://crudata.uea.ac.uk/cru/data/hrg/.

Methods

The phenology metrics, including the start of season (SOS), end of season (EOS), length of season (LOS), and peak of season (POS), were assessed in different climate zones. The method employed in this study is a modified dynamic (Optimal) threshold method developed by Huang *et al*. (2019), derived from the dynamic threshold method initially proposed by White *et al*. (1997). As illustrated in Figure 2, the amplitude used in recovering the SOS is denoted as *g1*, representing the difference between c and the lowest NDVI value on the left side. Similarly, *g2* represents the amplitude used to retrieve the EOS, calculated as the NDVI minimum value on the right side minus the NDVI maximum value of the growing season. The calculations for SOS and EOS thresholds are summarized in Equations (1 and 2),

$$(NDVI_{SOS} \geq \text{a} + NDVI_{Thrd} \times \text{g1}) \quad (1)$$

$$(NDVI_{EOS} \leq \text{b} + NDVI_{Thrd} \times \text{g2}) \quad (2)$$

In this work, a 20% threshold was adopted to ensure that $NDVI_{SOS} \leq c$, $NDVI_{EOS} \leq c$, and $NDVI_{Thrd} \leq 100\%$ are always satisfied. The Peak of Season (POS) is determined at the value of c, while the Length of Season (LOS) is calculated as the difference between EOS and SOS.

The relationship between NDVI and climate variables was ascertained using the cross-correlation coefficient at different time lags. The cross-correlation ($r_{xy}(\tau)$) formula is given by

$$r_{xy}(\tau) = \frac{\sum_{t=1}^{n-\tau}(x_t-\bar{x})(y_{t+\tau}-\bar{y})}{\sqrt{\sum_{t=1}^{n}(x_t-\bar{x})^2 \sum_{t=1}^{n}(y_t-\bar{y})^2}} \quad (3)$$

Where τ is the time lag, x_t and y_t represent the NDVI and climate variables at time *t*, $\bar{x}$ and $\bar{y}$ are the mean values of x_t and y_t respectively, and n is the length of data records.

The rate of shift in vegetation phenology (RPSH) of the various zones was assessed using Equation 4 (Wang *et al*., 2016)

$$RPSH = \frac{n \times \sum_{i=1}^{n} i \times Doy_i - \sum_{i=1}^{n} i \sum_{i=1}^{n} Doy_i}{n \times \sum_{i=1}^{n} i^2 - \left(\sum_{i=1}^{n} i\right)^2} \quad (4)$$

Where n is the total number of years and Doy_i is the seasonal phenology (EOS, SOS, POS, LOS) for year i (i is from 1 to n).

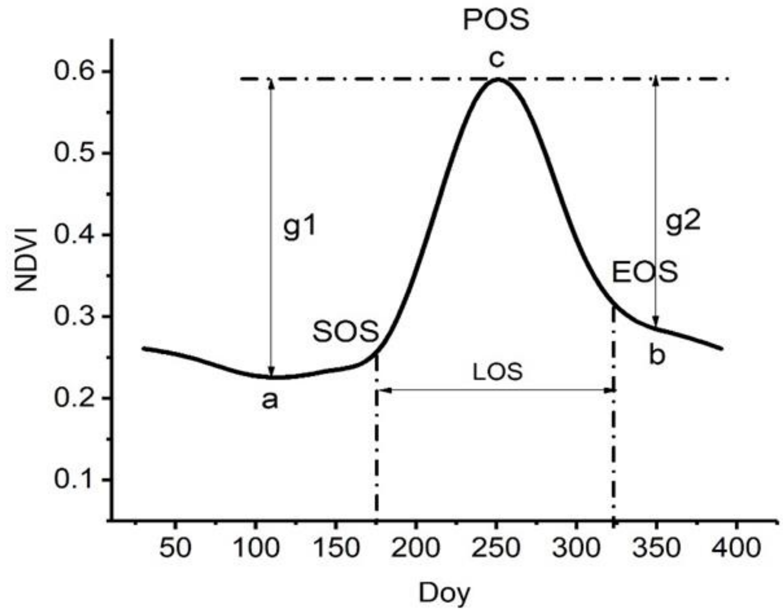

Figure 2 (a) Dynamic threshold approach before (a) and after modification (b), with the normalized difference vegetation index (NDVI) represented on the y-axis and the Day of Year (DOY) on the x-axis.

RESULTS AND DISCUSSION

Mean NDVI in different climate zones

Figure 3 shows the mean annual NDVI from 2001 to 2022 across different vegetation zones. The results reveal high fluctuation in vegetation over the years in these zones. High (low) NDVI values, as observed in Af, Am, Aw, BSh, BWh, Csb, were 0.618 (0.506), 0.624 (0.564), 0.542 (0.513), 0.365 (0.317), 0.3368 (0.304), and 0.642 (0.601) in 2020 (2019), 2008 (2015), 2019 (2015), 2022 (2009), 2020 (2002), and 2019 (2012), respectively. The NDVI standard deviation (std) was 0.032, 0.017, 0.008, 0.013, 0.016, and 0.013 for Af, Am, Aw, BSh, BWh, and Csb, respectively. This suggests high and low annual NDVI variability in Af and Aw climate zones respectively from 2001 to 2022. Additionally, results from this study (Figure 3) indicate that annual NDVI decreased in Am and Aw at -0.0002 and -0.0005 NDVI/yr, respectively. In contrast, in Af, BSh, BWh, and Csb, NDVI increased with slope values of 0.008, 0.0012, 0.0022, and 0.001 NDVI/yr, respectively. Meanwhile, the average NDVI over the country showed a positive trend of 0.008 NDVI/yr. The mean spatial distribution of NDVI for (a) DJF, (b) MAM, (c) JJA, (d) SON, and (e) MJJASON is presented in Figure 4. The results show that high clusters of NDVI were observed in JJA and SON seasons compared to DJF and MAM. The highest (lowest) pixels were observed in SON (DJF) than in other seasons, and high (low) clusters were visible in the southern (northern) parts of the country. Notably, Af and Am indicated high values due to the presence of thick vegetation, while BSh and BWh indicated low NDVI due to low vegetation cover in these regions. Similarly, the wet season average NDVI (MJJASON) appeared lower than the SON average, implying that wet season vegetation activity was lower than the SON average.

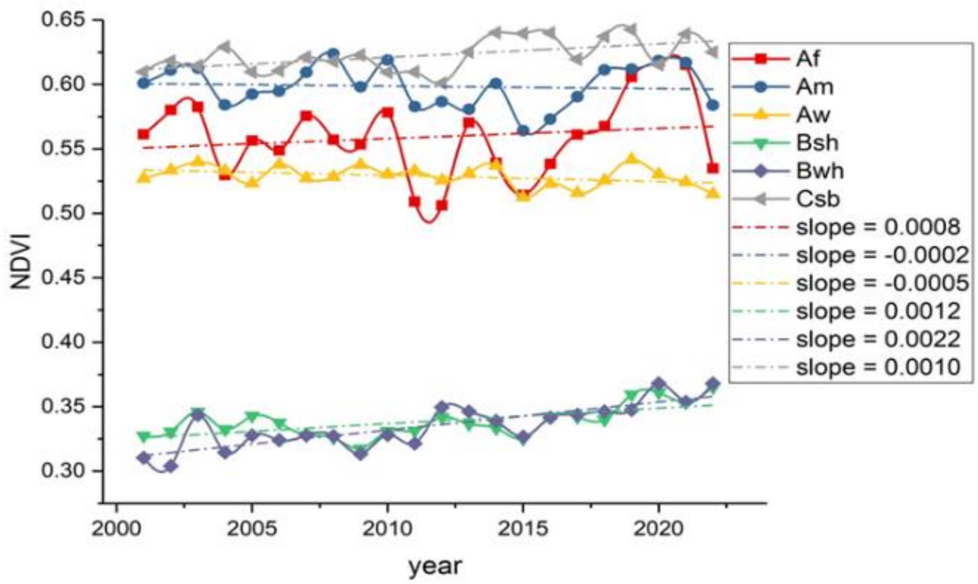

Figure 3: Mean NDVI in different climate zones

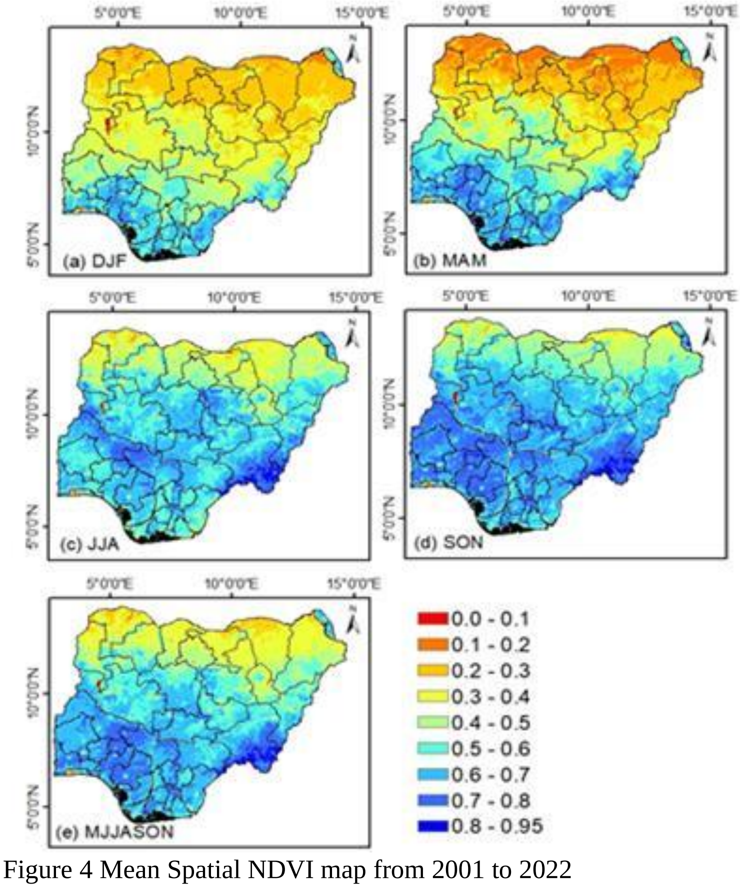

Figure 4 Mean Spatial NDVI map from 2001 to 2022

Annual Precipitation and Temperature distribution in study area

The annual distribution of precipitation and temperature in Nigeria from 2001 to 2022 is presented in Figure 5. The results show that precipitation is more variable over time than temperature across the climate zones. In the Af zone, the highest (lowest) values of precipitation and temperature were 217.8 (205.4) mm and 26.4 (25.8) °C, occurring in 2006 (2012) and 2021 (2012), respectively. In the Am zone, the highest (lowest) precipitation and temperature values were 212.8 (194.7) mm and 27.0 (26.5) °C in 2006 (2009) and 2021 (2012), respectively. In the Aw zone, the highest (lowest) precipitation and temperature values were 114.5 (89.0) mm and 27.6 (26.9) °C in 2019 (2011) and 2010 (2001), respectively. In the BSh zone, the highest (lowest) precipitation and temperature values were 73.5 (46.3) mm and 28.3 (27.9) °C in 2020 (2021) and 2018 (2022), respectively. In the BWh zone, the highest (lowest) precipitation and temperature values were 52.1 (25.0) mm and 29.7 (28.4) °C in 2012 (2021) and 2010 (2022), respectively. In the Csb zone, the highest (lowest) precipitation and temperature values were 150.0 (124.6) mm and 23.5 (22.8) °C in 2016 (2011) and 2016 (2001), respectively. Findings show that precipitation (temperature) decreased (increased) at -0.249 mm/yr (0.016 °C/yr) in Af from 2001 to 2022. In the Am zone, precipitation (temperature) decreased (increased) at -0.339 mm/yr (0.016 °C/yr), while precipitation and temperature increased at 0.103 mm/yr and 0.007 °C/yr, respectively, in the Aw zone. Also, precipitation (temperature) increased (decreased) at 0.248 mm/yr (-0.003 °C/yr) in the BSh zone. In the BWh, precipitation (temperature) increased (decreased) with a slope of 0.300 mm/yr (-0.009 °C/yr), while in the Csb zone, precipitation decreased in slope (-0.103 mm/yr), whereas temperature increased in slope (0.009 °C/yr) from 2001 to 2022. The mean monthly distribution of NDVI, precipitation, and temperature in the study area is illustrated in Figure 6. The results show that precipitation was higher in MAM, JJA, and SON than DJF across the climate zones. The month with the highest precipitation in all the climate zones was September. In contrast, peak values of precipitation were observed in August for BSh and BWh. Arguably, Af, Am, and Csb had the highest precipitation while BWh and BSh observed the lowest precipitation (Figure 6). In Af and Am, the NDVI signal correlates more with temperature during the growing season than precipitation. In contrast, the NDVI signal correlates more with precipitation than temperature in Aw, BSh, BWh, and Csb climate zones. Findings from Figure 6 showed that temperature reaches its peak at SOS (some degrees above normal) and EOS (some degrees below normal). From Figure 6, temperature indicated a bimodal distribution of values in all the climate zones. Generally, the first and second peaks are between April and October for BSh and BWh. In contrast, Af and Am indicated the first and second peaks in February and November, respectively. Also, for Aw and Csb, the first and second peaks occurred in March and November, respectively. Specifically, BWh and BSh showed higher temperatures during the MAM, JJA, and SON seasons, while Csb had the lowest temperatures during the growing season. During DJF, Af, Am, and Aw climate zones observed higher temperatures compared to the other climate zones.

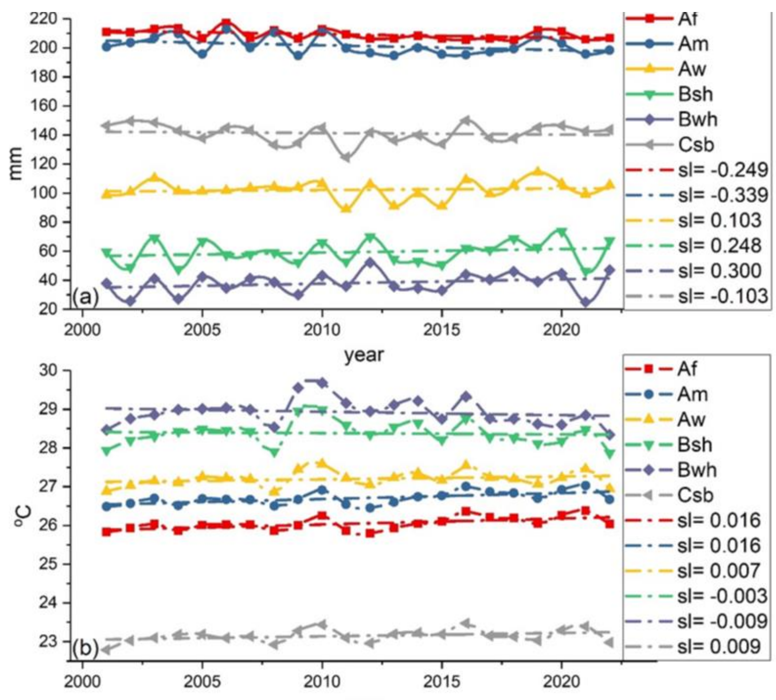

Figure 5: Annual distribution of (a) precipitation and (b) temperature from 2001 to 2022 across the different climate zones

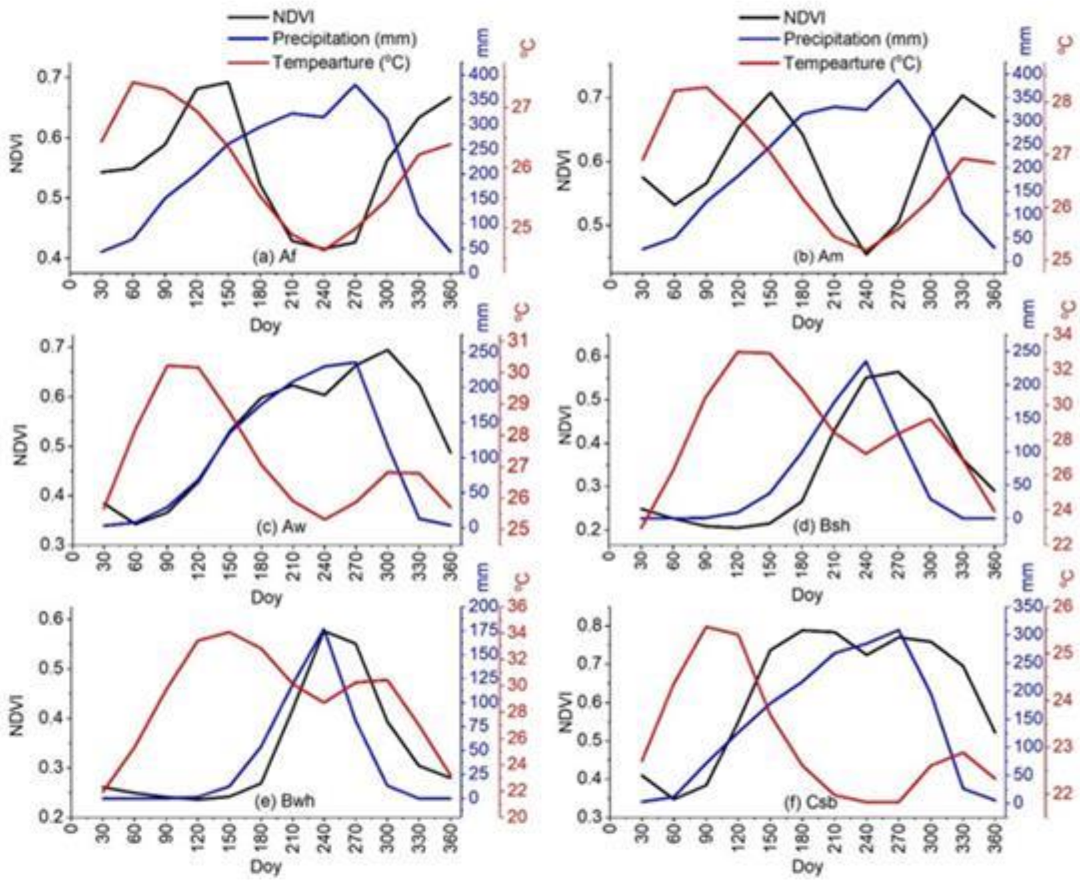

Figure 6: Mean Monthly Distribution of NDVI, Precipitation and Temperature from 2001 to 2022 across the climate zones

Cross Correlation analysis between NDVI and Climate variables (Precipitation and Temperature)

The cross-correlation analysis between NDVI and climate parameters is presented in Figure 7. The analysis was achieved using Equation 3. Results showed that the NDVI versus temperature indicated the maximum correlation observed at zero lags for all climate zones. Similarly, NDVI versus precipitation indicated the maximum correlation at zero lags in Af and Am, while the maximum correlation was observed at +1 lag in Aw, BSh, BWh, and Csb. This suggests that NDVI lags precipitation by 1 month in Aw, BSh, BWh, and Csb but is clearly in phase with precipitation in Af and Am. Arguably, the primary climate condition that affects vegetation growth change in Af and Am is temperature. In contrast, precipitation is the primary climate parameter that influences NDVI growth in Aw, BSh, BWh, and Csb. This work corroborated the findings of Igbawua et al. (2016), whose results similarly indicated that precipitation is the primary climate variable influencing changes in vegetation growth in Nigeria. The findings also aligned with those of Workie and Debella (2018), who identified a one-month lag time between NDVI and precipitation in Ethiopia.

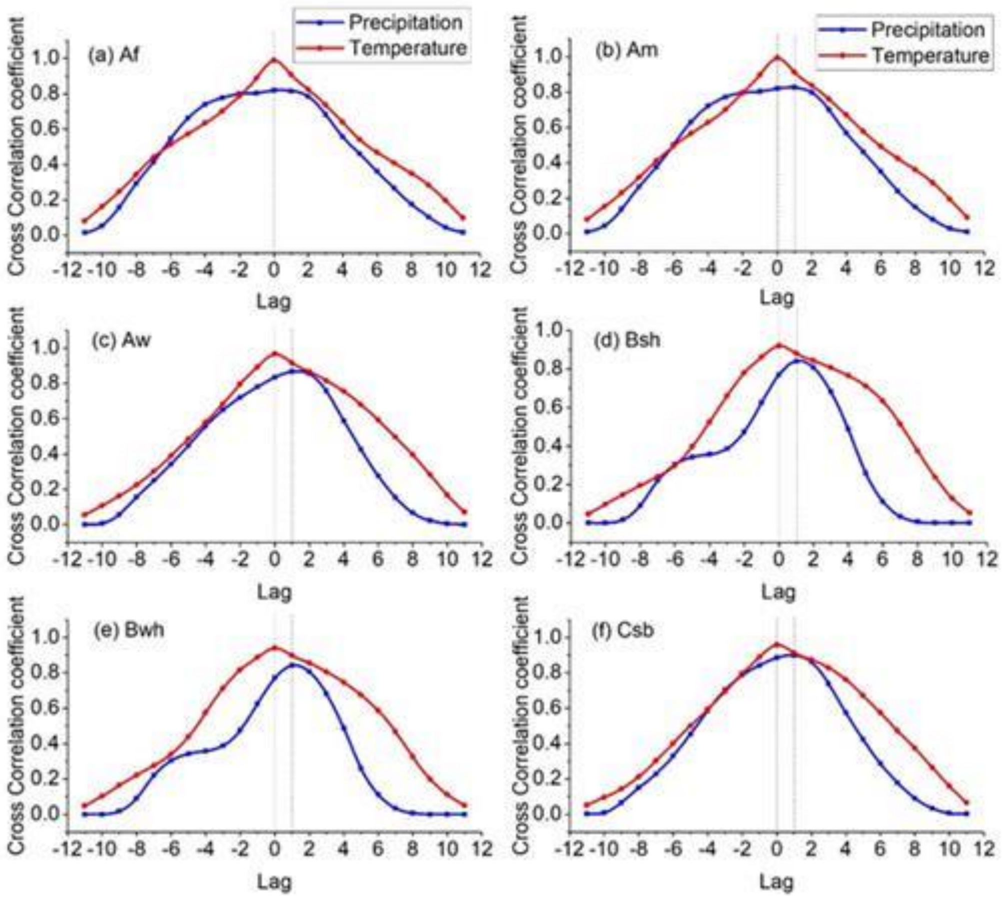

Figure 7: Cross correlation Analysis between NDVI and climate variables (precipitation and temperature)

Phenology Extraction using threshold method

Figure 8 shows the extracted phenological metrics across the seasons in Nigeria using the Optimal Threshold method given by Equations 1 and 2. Results show that the Day of Year (DOY) for Start of Season (SOS) and End of Season (EOS) appearance in Af, Aw, Am, BSh, BWh, and Csb was 80 (360), 83 (360), 115 (350), 183 (338), 190 (315), and 102 (355), respectively. Meanwhile, the seasons attained their Peak of Season (POS) at 140, 150, 300, 260, 250, and 190 for Af, Am, Aw, BSh, BWh, and Csb, respectively, with a length of season (LOS) as 280, 277, 235, 155, 125, and 253, respectively. The results showed that the Af (BWh) climate zone indicated the longest (shortest) season length, and longer zones with larger Length of Season (LOS) experienced delayed End of Season (EOS) and/or early onset of the season. Furthermore, Af climate seasons start earlier and finish later than those in the other climate zones. These findings corroborate the research by Igbawua *et al.* (2023), who also noted shorter seasons in the arid (Sahel) and longer seasons in the moonson and forest regions (Humid zone). of the study area.

The rate of phennology change illustrating how early or delayed the season might appear in each climate zone was analyzed using Equation 4 and results presented in Table 1. A positive (negative) value indicates how delayed (early), the season appears within the study time range. Findings show that SOS indicated a negative value suggesting how early the seasons have appeared from 2001 to 2022 in Af, Aw, BWh, and Csb at the rate of -1.2, -0.4, -0.3, and -0.5 days/year while a negative value of RPSH in Am indicated delayed SOS at 0.6 days/yr. In contrast, the SOS in BSh showed a value of 0 for RPSH which indicates no shift or change in SOS from 2001 to 2002. For EOS, Af, Am, Aw, and Csb remianed unchaged with RPSH value of 0. Meanwhile, BSh and BWh showed a delayed EOS with RPSH value of 0.2 and 0.6 days/yr respectively. Moreso, the POS in Af appeared early with RPSH value of -1.4 days/yr but delayed in Am, Aw, BSh, BWh, and Csb with RPSH value of 1.1, 0.4, 0.1, 0.2, and 0.4 days/yr respectively. Similarly, the LOS expanded in Af, Aw, BSh, BWh, and Csb with RPSH value of 1.2, 0.4, 0.2, 0.9, and 0.5 days/yr. In contrast, LOS in Am indicated an RPSH value of -0.6 days/yr suggesting shortening of season length. In this study, early Start of Season (SOS) in Af, Aw, BWh, and Csb could be linked to slight increases in MAM temperatures (see Figures 9). Wang *et al*. (2019) also reported that high spring (MAM) temperatures trigger earlier leaf onset, which could lead to a prolonged growing season. Similarly, Liu *et al*. (2020) reported that delays in SOS may be attributed to cool temperatures. However, in this study, delays in SOS were not a result of cooling MAM temperatures (see Figure 9).

The findings from this study show that in Af and Am, precipitation is high throughout the year, and the limiting factor is temperature, which is needed for warmth. Similarly, in Aw, BSh, BWh, and Csb, temperatures are high, while precipitation ranges from moderate to low. The limiting factor influencing vegetation growth is precipitation. Chen *et al*. (2023) assert that temperature directly affects EOS and SOS, while precipitation indirectly affects SOS and EOS. Documented evidence by Cerlini *et al*. (2022), Cui *et al*. (2022) and Igbawua *et al*. (2023) has noted the effects of climate change on phenology.

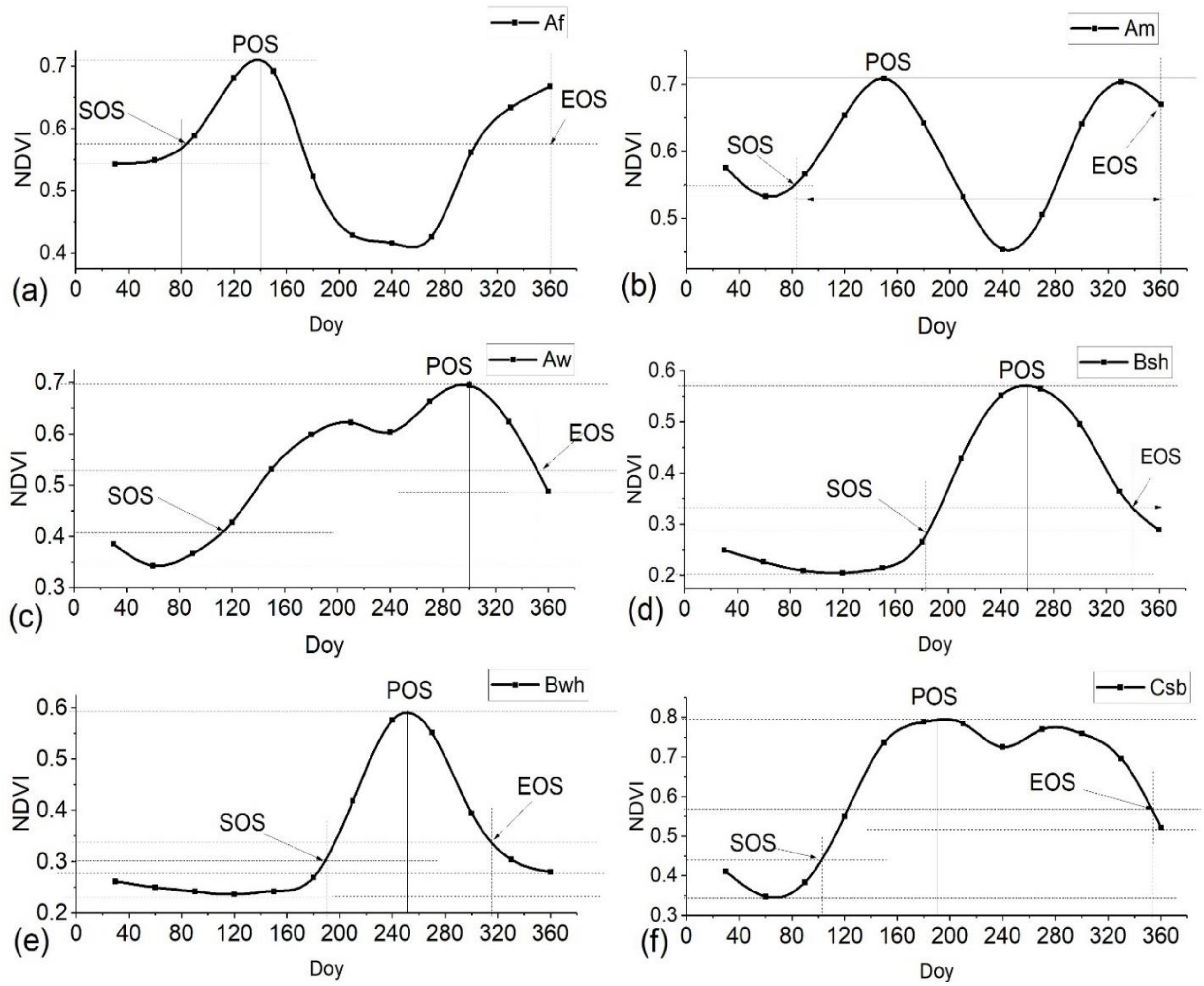

Figure 8: Phenology extraction using Optimal threshold method

Table1: Rate of Phenology shift (RPSH)

Koppen	SOS	EOS	POS	LOS
Af	-1.2	0.0	-1.4	1.2
Am	0.6	0.0	1.1	-0.6
Aw	-0.4	0.0	0.4	0.4
Bsh	0.0	0.2	0.1	0.2
Bwh	-0.3	0.6	0.2	0.9
Csb	-0.5	0.0	0.4	0.5

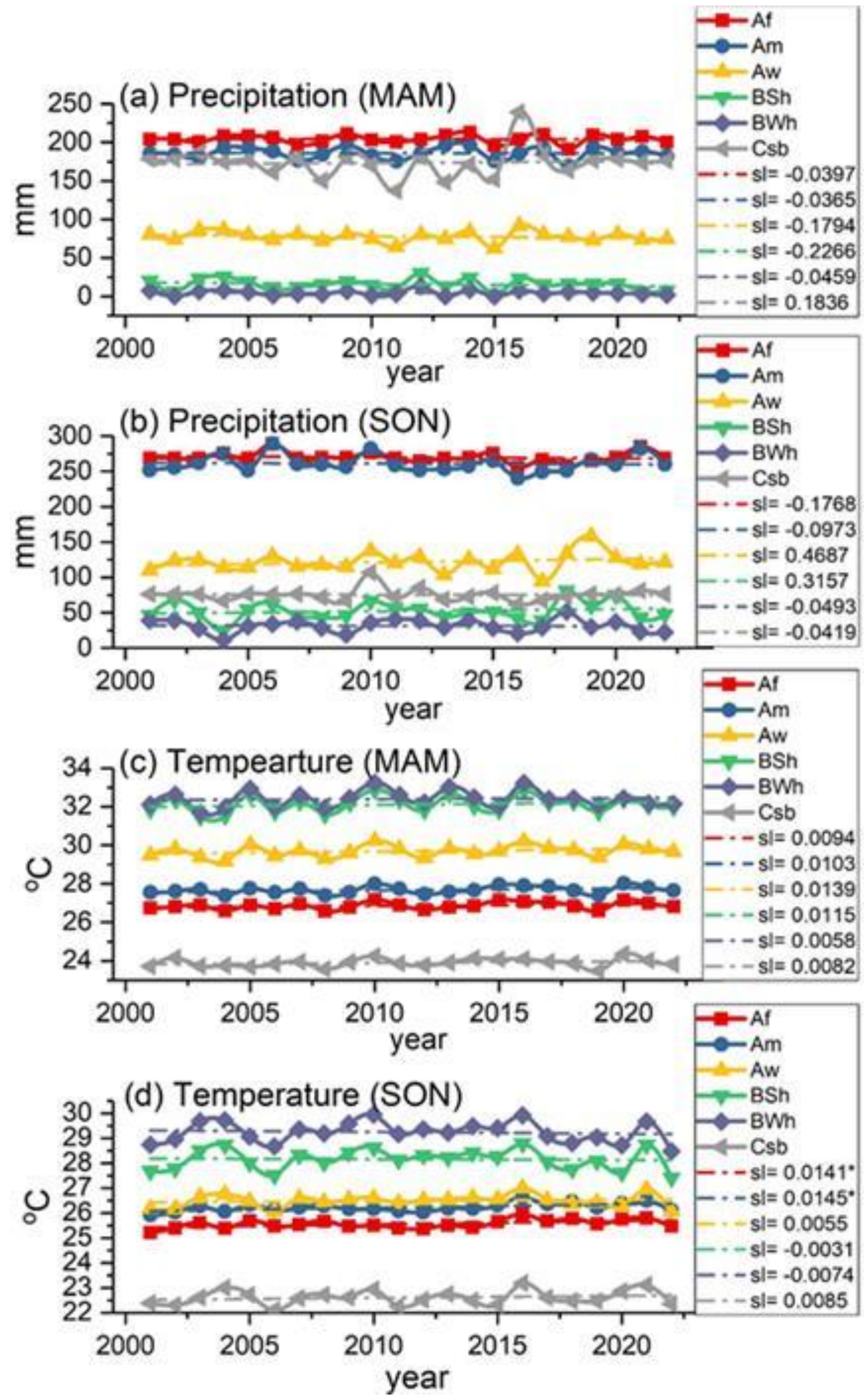

Figure 9 (a-b) MAM and SON season precipitation and (c-d) MAM and SON season temperature

CONCLUSION

The modified dynamic (optimal) threshold method presents a robust and effective approach for determining the onset and end of the growing season with high accuracy level. By incorporating dynamic adjustments to threshold values based on environmental conditions, this method offers improved accuracy and reliability compared to static threshold approaches. Through the analysis of relevant environmental variables such as temperature, precipitation, and vegetation indices, the modified dynamic (optimal) threshold method adopted in this study captured the nuanced variations in the timing of plant growth initiation and cessation. This adaptability is particularly valuable in Nigeria given the diverse climatic patterns and vegetation dynamics in spatio-temporal terms. Moreover, the optimization component of the method ensured that the selected thresholds are tailored to specific local conditions, enhancing the precision of growing season delineation. This adaptability is crucial for monitoring shifts in growing season patterns due to climate change or land use alterations as widely recorded in different parts of Nigeria. Overall, the modified dynamic (optimal) threshold method provides a valuable tool for researchers, policymakers, and stakeholders involved in agriculture, ecology, and climate science. Its ability to accurately identify the onset and end of the growing season contributes to improved understanding and management of ecosystems, agricultural productivity, and climate change impacts. However, further research and validation efforts will continue to refine and enhance the applicability of this method across different spatial and temporal scales for vegetation phenological interrogation in Nigeria.

REFERENCES

Atzberger, C., Eilers, P.H.C. (2011) A time series for monitoring vegetation activity and phenology at 10-daily time steps covering large parts of South America. *Int. J. Digital Earth*, 4 (5):365–386. https://doi.org/10.1080/17538947.2010.505664

Atkinson, P.M., Jeganathan, C., Dash, J. and Atzberger, C. (2012). Inter-comparison of four models for smoothing satellite sensor time-series data to estimate vegetation phenology. *Remote Sens. Environ*, 123:400–417. https://doi.org/10.1016/j.rse.2012.04.001

Beck, P.S.A., Atzberger, C., Høgda, K.A. and Skidmore, A.K. (2006). Improved Monitoring of Vegetation Dynamics at Very High Latitudes: A New Method Using MODIS NDVI. *Remote Sensing of Environment*, 100(3):321-334. https://doi.org/10.1016/j.rse.2005.10.021

Cerlini, P.B., Saraceni, M., Orlandi, F., Silvestri, L. and Fornaciari, M. (2022). Phenological response to temperature variability and orography in Central Italy. *Int J Biometeorol*, 66:71–86. https://doi.org/10.1007/s00484-021-02190-1

Chen, X., & Zhang, Y. (2023). The impact of vegetation phenology changes on the relationship between climate and net primary productivity in Yunnan, China, under global warming. *Frontiers in plant science*, 14: 1248482. https://doi.org/10.3389/fpls.2023.1248482

Cui, X., Xu, G., He, X. and Luo, D. (2022). Influences of Seasonal Soil Moisture and Temperature on Vegetation Phenology in the Qilian Mountains. REMOTE SENS., 14: 3645. https://doi.org/10.3390/rs14153645

Curnel, Y., Oger, R. (2006). Agrophenology indicators from remote sensing: state of the art. In Proceedings of ISPRS Archives XXXVI-8/W48 Workshop proceedings: Remote sensing support to crop yield forecast and area estimates, Stresa, Italy, 30 Nov–1 Dec 2006; pp. 31–38. https://www.isprs.org/proceedings/XXXVI/8-W48/31_XXXVI-8-W48.pdf

Duchemin, B.T., Goubier, J.M. and Courrier, G. (1999). Monitoring phenological key stages and cycle duration of temperate deciduous forest ecosystems with NOAA/AVHRR data. *Remote Sens. Environ*., 67:68–82. https://doi.org/10.1016/S0034-4257(98)00067-4

Fischer, A. (1994) A model for the seasonal variations of vegetation indices in coarse resolution data and its inversion to extract crop parameters. *Remote. Sens. Environ*., 48:220–230. https://doi.org/10.1016/0034-4257%2894%2990143-0

Fisher, J.I., Mustard, J.F. and Vadeboncoeur, M.A. (2006). Green leaf phenology at Landsat resolution: Scaling from the field to the satellite. *Remote Sens. Environ*. 100:265–279. https://harvardforest1.fas.harvard.edu/publications/pdfs/Fisher_RemoteSensEnviron_2007.pdf

Huang, X., Liu, J., Zhu, W., Atzberger, C. and Liu, Q. (2019). The Optimal Threshold and Vegetation Index Time Series for Retrieving Crop Phenology Based on a Modified Dynamic Threshold Method. REMOTE. SENS., 11(23): 2725. https://doi.org/10.3390/rs11232725

Igbawua, T., Zhang, J., Chang, Q. and Yao, F. (2016). Vegetation dynamics in relation with climate over Nigeria from 1982 to 2011. *Environmental Earth Sciences*, 75:1-16. https://link.springer.com/article/10.1007/s12665-015-5106-z

Igbawua, T., Abiem, L.T., tsor, J.O., Adagba, G. and Egbe, S. (2023) Assessment of Start and End of Growing Seasons in different Ecological Zones of Nigeria Using Satellite Data, *Nigerian Annals of Pure and Applied Sciences*, 6(1):154-171. DOI:10.5281/zenodo.7338397

Jeong, S.J., Ho, C.H., Kim, J. and Levis, S. (2011). Impact of vegetation feedback on the temperature and its diurnal range over the Northern Hemisphere during summer in a 2_ CO_2 climate. *Climate Dynamics*, 37: 821–833.

https://link.springer.com/article/10.1007/s00382-010-0827-x

Jonsson, P., Eklundh, L. (2002). Seasonality extraction by function fitting to time-series of satellite sensor data. IEEE Trans. *Geosci. Remote. Sens*., 40:1824–1832. doi: 10.1109/TGRS.2002.802519

Li, H., Li, F.Y., Guo, J. and Gao, X. (2023). An improved dynamic threshold method for determining the start of the vegetation greening season in remote sensing monitoring: The case of Inner Mongolia. *Ecological Informatics*, 78 (102378). https://doi.org/10.1016/j.ecoinf.2023.102378

Liu, L., Zhang, X. (2020) Effects of temperature variability and extremes on spring phenology across the contiguous United States from 1982 to 2016. *Sci Rep*, 10:17952. https://doi.org/10.1038/s41598-020-74804-4

Lloyd, D. (1990). A phenological classification of terrestrial vegetation cover using shortwave vegetation index imagery. *Int. J. Remote. Sens*., 11:12, 2269-2279, DOI: 10.1080/01431169008955174

Miao, L., Jiang, C., Xue, B., Liu, Q., He, B. and Nath, R. (2014). Vegetation dynamics and factor analysis in arid and semi-arid Inner Mongolia. *Environmental Earth Sciences*. 73:2343–2352. https://doi.org/10.1007/s12665-014-3582-1

Reed, B.C., Brown, J.F., Vanderzee, D., Loveland, T.R., Merchant, J.W. and Ohlen, D.O. (1994) Measuring phenological variability from satellite imagery. *J. Veg. Sci*., *5*(5):703-714. https://doi.org/10.2307/3235884

Sakamoto, T., Yokozawa, M., Toritani, H., Shibayama, M., Ishitsuka, N. and Ohno, H. (2005) A crop phenology detection method using time-series MODIS data. *Remote Sens. Environ.*, 96(3-4):366-374. https://doi.org/10.1016/j.rse.2005.03.008

Wang, S., Yang, B., Yang, Q., Lu, L., Wang, X. and Peng, Y. (2016). Temporal Trends and Spatial Variability of Vegetation Phenology over the Northern Hemisphere during 1982-2012. *PLoS One*. 11(6): e0157134. https://doi.org/10.1371/journal.pone.0157134

Wang, Y., Luo, Y. and Shafeeque, M. (2019). Interpretation of vegetation phenology changes using daytime and night-time temperatures across the Yellow River Basin, China. *Science of The Total Environment.* 693, https://doi.org/10.1016/j.scitotenv.2019.07.359

White, M.A., Thornton, P.E. and Running, S.W. (1997). A continental phenology model for monitoring vegetation responses to interannual climatic variability. *Global Biogeochem. Cycles*, 11(2):217-234. doi: 10.1029/97GB00330

Workie, T. G. and Debella, H. J. (2018). Climate change and its effects on vegetation phenology across ecoregions of Ethiopia. *Global Ecology and Conservation*, 13:e00366. https://doi.org/10.1016/j.gecco.2017.e00366

Zhang, X., Friedl, M.A. Schaaf, C.B., Strahler, A.H., Hodges, J.C.F., Gao, F., Reed, B.C. and Huete, A. (2003) Monitoring vegetation phenology using MODIS. *Remote Sens. Environ*., 84:471–475. https://doi.org/10.1016/S0034-4257(02)00135-9